Universidad del País Vasco Euskal Herriko Unibertsitatea

ZIENTZIA ETA TEKNOLOGIA FAKULTATEA
FACULTAD DE CIENCIA Y TECNOLOGÍA

Gradu Amaierako Lana / Trabajo Fin de Grado
Biokimika eta Biologia Molekularreko Gradua / Grado en Bioquímica y Biología Molecular

Unravelling the link between PGC1α and interferon signaling in prostate cancer

Egilea/Autor:

Ander Uribarri García

Zuzendaria/Directora:

Verónica Torrano Moya

Zuzendarikide/Co-Director:

Antonio Gomez Muñoz

Leioa, 2021ko ekainaren 17a / Leioa, 17 de junio de 2021

Contents:

Acknowledgements: Thanks to everyone in the laboratory and specially Alice for being so patient and helping us so much during this project. Thanks to Aintzane and Aroa for sharing this first experience together. Lastly, thanks to Vero for giving me this opportunity and always being there for us.

Unravelling the link between PGC1α and interferon signaling in prostate cancer.

Graphical Abstract:

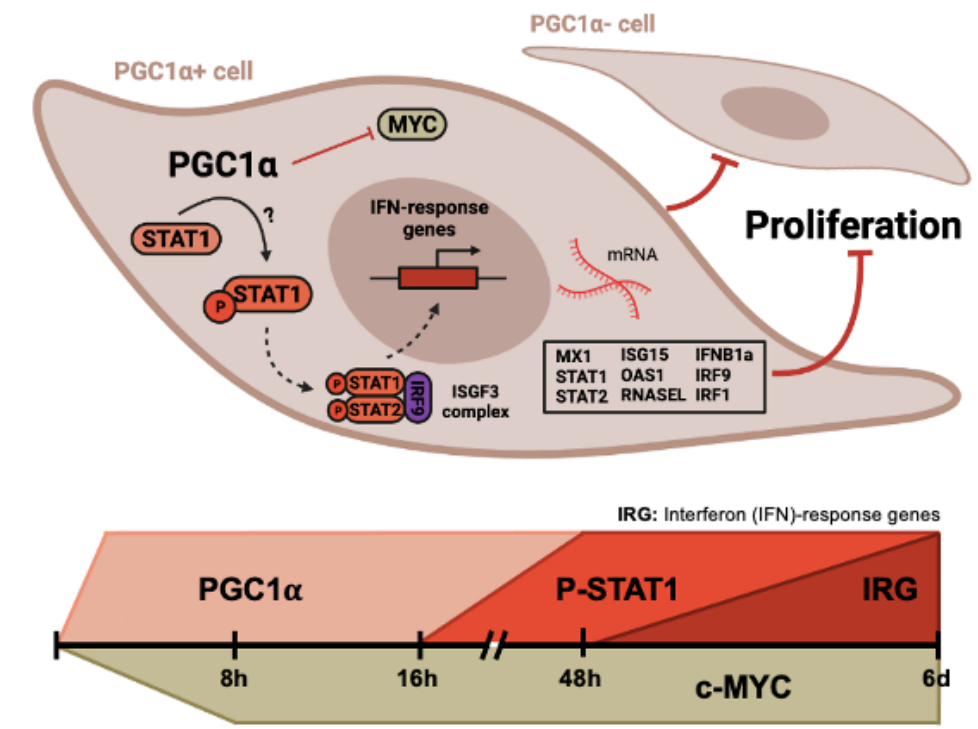

Image created using BioRender

Abstract:

Prostate cancer (PCa) is the second most diagnosed cancer among males worldwide. Due to the current molecular markers used in clinic there is an overdiagnosis and patient overtreatment, revealing the need for biomarkers and gene signatures capable of stratifying patients, distinguishing aggressive prostate tumors from the indolent ones. Our laboratory has previously reported a master co-regulator of PCa metabolism capable of exerting a tumor and metastasis suppressive response: the peroxisome proliferator-activated receptor gamma co-activator 1 (PGC1α). PGC1α has been shown to prevent tumor growth, metastasis and invasion in PCa, associated with the downregulation of c-MYC. Given the unknown molecular mechanisms driving the biological effects of PGC1α and a recent RNA-sequencing experiment carried out in our laboratory, we hypothesize that the interferon transcriptional program upregulated by PGC1α drives its tumor suppressive activity. Interferons (IFNs) are cytokines greatly studied in cancer due to their ability to directly and/or indirectly modulate tumorigenesis. However, their role on PCa is not completely studied. In this context, we have characterized the PGC1α-driven phosphorylation of STAT1 and the subsequent upregulation of the IFN transcriptional program in (i) PGC1α expressing and (ii) IFN-β treated PCa cells. Lastly, in co-cultures assays, we have approached the study of the anti-proliferative effect of the cell communication between PGC1α expressing and non-expressing PCa cells. Altogether, we consider the present work a first approach to studying the link between IFN pathway and the tumor suppressive properties of PGC1α in PCa cells, offering potential for new therapeutic targets and strategies.

1. Introduction

Prostate cancer (PCa) is the second most frequent diagnosed cancer among males worldwide, with an estimated 1,400,000 cases and 375,000 deaths in 2020. In developed countries, PCa shows the highest incidence among cancer types in men, representing the third cause of death by cancer in the gender[1]. Prostate-specific antigen (PSA) is the usual molecular marker used for the detection and monitoring of PCa. However, PSA screening has been highly controversial, due to the detection of inherently benign tumors and the fact that PSA levels can be influenced by other physiological factors. This results in an overdiagnosis and patient overtreatment, which questions the effectiveness of this biomarker by itself as an early detection tool[2].

PCa treatment ranges from active surveillance to a combination of surgery, radiotherapy, chemotherapy and/or androgen deprivation therapy (ADT). Low-risk cancers are usually handled by active surveillance, while high-risk cancers (primary tumors) are managed with a more aggressive treatment, including surgery and radiotherapy. The major challenge comes to intermediate-risk tumors, due to the inability to differentiate between aggressive and non-aggressive cancers. A key feature of PCa is hormone responsiveness and the standard care for advanced PCa is ADT[2,3]. ADT can be approached by surgical castration, or more commonly, by chemical castration, with drugs targeting androgen receptor signaling. Although the majority of the patients respond well to ADT, resistance can develop, resulting in castration-resistant PCa. Considering that metastatic disease is the leading cause of death in PCa, research is focusing on the development of more accurate detection techniques and biomarkers that can effectively distinguish between aggressive and indolent forms of PCa in the earliest stages of the disease[3].

It is well accepted that the uncontrolled growth of tumors is not only supported by a deregulation of the cell proliferation mechanisms, but also by reprogramming the energy metabolism, an emerging hallmark of cancer[4]. Integrating computational biology, murine models and high throughput OMICs, our laboratory group has formerly reported that the peroxisome proliferator-activated receptor gamma co-activator 1 alpha (PGC1α), a master co-regulator of PCa metabolism, is central for the progression of the disease[5]. PGC1α is preferentially expressed in tissues with high oxidative capacities (such as skeletal muscle or brown adipose tissue) and interacts with a variety of transcription factors (TFs), serving as a pleiotropic regulator of the cell metabolism. The N-terminal of PGC1α contains several leucine-rich motifs (LXXLL), crucial for the interaction with the different TFs[6]. Some of these TFs include the estrogen-related receptor alpha (ERRα), retinoid receptors, nuclear respiratory factor-1 and -2 (NRF-1, NRF-2) or peroxisome proliferator-activated receptors (PPARα, PPARβ, PPARγ)[7]. PGC1α partnering with these TFs carries out its main biological functions: mitochondrial biogenesis, fatty acid oxidation and muscle fiber regeneration. The expression and activity of PGC1α is controlled by physiological and environmental stimuli, modulating the energy metabolism of the cell[6,7]. Therefore, it comes as no surprise the implication of this co-regulator in cancer, since tumor cells continuously adapt their metabolism in response to their microenvironment.

The role of PGC1α is tumor type and context-specific and can be discordant in different scenarios. In breast cancer, metastatic cells rely on PGC1α for metastatic dissemination, enhancing oxidative phosphorylation[8]. Moreover, PGC1α is overexpressed in breast cancer cells that metastasize to lung and bone[9]. Nonetheless, the

expression of PGC1α exerts an anti-proliferative effect in PCa, preventing tumor growth and metastatic dissemination[5, 10].

The loss of the expression of PGC1α in prostate cancer is associated with a metabolic rewiring, towards the activation of anabolism at the expense of a reduction in the catabolism. At the transcriptional level, the decrease in PGC1α expression defines a gene signature that is progressively downregulated in PCa primary tumors and metastasis, presenting prognostic potential for the stratification of patients[5].

The role of the oncogenic protein c-MYC has been widely studied in human tumors. Enhanced MYC expression has been shown to reprogram cellular metabolism, sustaining a high rate of proliferation in cancer cells[11]. In PCa murine models, the expression of human *MYC* has been shown to be an initiating event in the development of murine prostate tumors, highlighting the importance of this TF in the disease[12]. Furthermore, a recent study from our laboratory has demonstrated that the expression of PGC1α decreases invasive capacities in PCa cells through cytoskeletal remodeling, together with the inhibition of integrin β1, β4 and c-MYC[10]. However, the exact molecular mechanisms driving the biological effects of PGC1α are still unknown.

Interferons (IFNs) are pleiotropic cytokines that serve as a defense mechanism against viral infections[13,14]. Nonetheless, IFNs have been extensively studied in cancer, due to their ability to regulate tumorigenesis in a direct or indirect way. IFN type I molecules (IFN-α and IFN-β) signal through the IFNAR1-IFNAR2 receptor dimer. After the ligand has bound, the receptor-associated kinases JAK1 and TYK2 are phosphorylated. These phosphorylated kinases serve as a docking and activation platform for the recruitment and downstream phosphorylation of STAT proteins. The canonical signaling complex for IFN type I signaling is a STAT1-STAT2-IRF9 complex (ISGF3 complex), which migrates to the nucleus and promotes the transcription of IFN-response genes[13]. Deciphering the role of IFNs in PCa is important owing to their tumor suppressive properties. Previous studies have shown that IFN type I cytokines upregulate the inhibitor of cell cycle progression p21[15] and exert an invasion-suppressor activity in PCa cells[16]. Furthermore, PCa cells engineered to produce IFN-β have shown to suppress angiogenesis, growth and metastasis in mouse models *in vivo*[17].

In this context, a recent RNA Sequencing (RNA-Seq) experiment carried out in our laboratory revealed an upregulation of the IFN signaling transcriptional program in response to PGC1α re-expression in PCa cells. In line, previous data from the lab have shown an increase of IFN-β in the secretome of PGC1α expressing PCa cells and that this secretome has an anti-proliferative effect. Therefore, in this work we aim to further elucidate the role of these cytokines and their associated signaling pathway in PCa cells.

2. Hypothesis and Objectives

Taking into account the preliminary data of the lab and given the unknown molecular mechanisms driving the biological effects of PGC1α, we hypothesize that this IFN transcriptional program drives PGC1α's tumor suppressive activity that ultimately could be transmitted in a paracrine manner to adjacent cancer cells. Therefore, in this work we ambitioned to: **(i)** characterize the PGC1α-driven IFN pathway in PCa cells, **(ii)** confirm the tumor suppressive activity of IFN signaling in PCa cells, and **(iii)** approach the extrinsic tumor suppressive activity of PGC1α in co-culture assays.

3. Materials and Methods

3.1. Cell lines and culture conditions:

Prostate cancer cell line PC3 was used in this work. These cells are epithelial cells derived from a bone metastasis of a grade IV prostatic adenocarcinoma from a Caucasian 62-year-old male. Previously in the lab, this cell line was modified to stably express the mouse *Pgc1a* gene with a doxycycline-inducible lentiviral vector (TRIPZ vector). This cell line, PC3 TRIPZ-HA-*Pgc1a* (from now on referred as PC3 PGC1α), in the presence of doxycycline in the medium overexpresses PGC1α. As control, PC3 cells transduced with TRIPZ empty vector (without the *Pgc1a* construct) were also used, PC3 TRIPZ. In the c-MYC exploratory experiments a third line was used, PC3 pLKO TetOn shMYC (PC3 shMYC), a modified PC3 cell line that in the presence of doxycycline expresses a validated shRNA against human *MYC*[18]. For the co-culture experiments a fourth cell line was used, PC3 TRIPZ-mCherry (PC3 mCherry), a modified PC3 cell line transduced with a TRIPZ vector containing the mCherry sequence, constitutively expressing the fluorescent protein mCherry.

All cell lines were cultured using Dulbecco's Modified Eagle Medium (1x) (DMEM) supplied with 10% inactivated Fetal Bovine Serum (FBS) (Gibco) and 1% Penicillin/Streptomycin (Gibco). Cell lines were grown at 37ºC in a humidified atmosphere of 5% CO_2. Cells were regularly cultured in 100mm dishes and split every 3-4 days, maintaining them below 80-90% density. For splitting and seeding, 0.25% trypsin-EDTA (1x) (Gibco) diluted 1:4 in Dulbecco's Phosphate Saline Buffer (1x) (DPBS) was used. For splitting or cell counting, cells were detached from the plates by incubating with the trypsin-EDTA solution for 4 minutes at 37ºC. Fresh DMEM was added for inactivation of the trypsin.

For cell counting, the resuspended cells were diluted 1:2 in Trypan Blue Dye 0.4% and 10 µL were loaded in the Neubauer chamber. The viable cells (not stained with the dye) were counted by optical microscopy. Cell counting was performed at least twice for each sample to obtain a more accurate count.

Co-cultures: For co-culture experiments different cell mixtures were prepared as represented in Table 1. The growth rate of each independent cell line was also measured.

Table 1. The three different co-culture conditions prepared for the growth curve and flow cytometry assays.

Co-culture condition	PC3 mCherry (%)	PC3 PGC1α or PC3 TRIPZ (%)
80:20	**80 %**	20 %
50:50	**50 %**	50 %
20:80	**20 %**	80 %

Doxycycline (Dox) was used at a final concentration of 0.5 µg/ml (Sigma #D9891). For the interferon experiments 3 different concentrations of human recombinant IFN-β (hIFN-β1a, Miltenyi Biotech) were used: 25, 125 and 250 pM. All the experiments were performed after 3 days of pre-induction with Dox of the cells, with the exception of interferon experiments and time-course experiments. The composition of the buffers used is presented in Supplementary Table 1.

3.2. Cellular experiments:

Cell growth analysis

To monitor cell growth, 10K cells/well were seeded in triplicate in 12-well plates for days 0 (seeding control), 3 and 6. In the interferon experiments, the day after seeding the medium was replaced with fresh medium with the different IFN-β concentrations. For fixation each well was washed with DPBS (1x) and 1 mL/well of formalin (10%) was added to the plates and stored at 4ºC until the end of experiment (day 6). For cell number quantification, formalin was discarded and cells were stained with crystal violet (0.1% in 20% methanol) for 45 minutes. After rinsing with water and air drying the plates, the precipitate was solubilized in 10% acetic acid. Resolubilized crystal violet was transferred to a 96 well-plate and absorbance was measured at 570 nm using the PowerWave XS Microplate Spectrophotometer (BioTek). The absorbance measured at days 3 and 6 was normalized by the absorbance at day 0, obtaining the growth fold-change relative to day 0.

Flow cytometry assays

In order to follow up the different cell percentages (%) in the co-culture conditions, 40K cells/well were seeded in duplicate in 6-well plates for days 0 (seeding control), 3, 6 and 9. On days 0, 3, 6 or 9, after medium was discarded, cells were washed with DPBS (1x), 250 µL of trypsin were added to each well and plates were incubated at 37ºC for 4 minutes. Cells were then resuspended with 1 mL DPBS (1x) and transferred to a separate Falcon 15 mL tube. Tubes were centrifuged (1500 rpm, 3 min, 4ºC) and the supernatant was discarded. Cell pellets were resuspended in 1 mL of DPBS (1x) and the centrifugation was repeated under the same conditions. The supernatants were removed, the cells were resuspended with 500 µL of DPBS (1x) and transferred to a flow cytometer tube that were kept on ice.

Selection of the cell population of interest was done using the representation of the forward scattered light (FSC) vs. side scattered light (SSC). FSC intensity is proportional to the cell size, while SSC provides information about the internal complexity of cells. The cytometer data was analyzed using the Flowing (Turku Bioscience) software. The constitutively expressed mCherry protein in PC3 mCherry cells allowed to divide the cell population into two different subgroups attending to the emitted fluorescence. The % of each subgroup was calculated as the counts of cells in that subgroup divided by the total counts of the cell population.

3.3. Molecular experiments:

Gene expression analysis

Between 75-100K cells/well were seeded in duplicate in 6-well plates and cells were collected after the indicated time points. Before RNA extraction, plates/wells were washes with DPBS (1x), snap-frozen in liquid N_2 and stored at -80ºC. Once all experiments were collected, RNA was extracted using the NucleoSpin RNA isolation kit from Macherey-Nagel (ref: 740955.240C). Final RNA concentration was measured in a Biodrop spectrophotometer and samples were stored at -20ºC. For cDNA synthesis 1 µg of total RNA was retrotranscribed. The mix of retrotranscription contained RNA (1 µg), the enzyme Thermo Scientific Maxima H Minus cDNA synthesis Master mix (5x) and RNase free water (up to final volume, 10 µL). The samples

were placed in a thermocycler and the following program was used: 10 minutes at 25ºC, 15 minutes at 50ºC and lastly 5 minutes at 85ºC. The resultant cDNA was diluted 1:10 in distilled water and kept at -20ºC.

Quantitative real-time PCR (qPCR) was performed in a QuantStudio 5 Real-Time PCR Instrument (384-Well Block) (Applied Biosystems). The program used for amplification was the following: 2 minutes at 50ºC and 10 minutes at 95ºC, followed by 40 cycles of 15 seconds at 95ºC and 1 minute at 60ºC. Quantification was carried out using TaqMan probes (Applied Biosystems) or SYBR Green (Roche).

TaqMan probes are specifically designed for the candidate gene and consist of a reporter and a quencher (which are attached to the 5' and 3' end of the probe, respectively). When these are released by the 5'-3' exonuclease activity of the DNA polymerase, the reporter's fluorescence is detected. SYBR Green is an intercalating dye that has a high binding affinity for double strand DNA (dsDNA). Once the dye binds to dsDNA its fluorescence increases and can be measured in the extension phase of each cycle. Given the nonspecificity of this last quantification method, a melting curve analysis is highly recommended. In both cases, the emitted fluorescence follows a sigmoidal increase and the threshold cycle (Ct) is used to calculate the initial DNA copy number[19].

For the TaqMan reaction, 3 µL of the diluted cDNA were mixed with 3 µL of the TaqMan Universal Master Mix II, with UNG (2x, Applied Biosystems), left and right primers at a final concentration of 200 nM and TaqMan probes at a concentration of 100 nM. For the SYBR Green reaction, 3 µL of the diluted cDNA were mixed with 3 µL of the FastStart Universal SYBR® Green Master (Roche) and left and right primers at a final concentration of 200 nM. All qPCR data presented were normalized using *GAPDH* (housekeeping gene) levels as reference. The primers used are presented in the Supplementary Table 2.

Protein analysis

Between 75-100K cells/well were seeded in duplicate in 6-well plates and cells were collected after the indicated time points. Before protein extraction, plates/wells were washes with DPBS (1x), snap-frozen in liquid N_2 and stored at -80ºC. Once all experiments were collected, cells were lysed using 75 µL/well of RIPA buffer. Lysates were transferred to Eppendorf tubes, kept for 20 minutes on ice and vortexed every 5 minutes. Samples were then centrifuged (15 000 g, 15 min, 4ºC) and the supernatant was collected. Protein quantification was carried out using Pierce™ BCA Protein Assay Kit (Thermo Fisher Scientific, 23225). A calibration curve was prepared using different concentration of Bovine Serum Albumin (BSA, 0.5-8 mg/mL) and 1 µL of the protein samples was mixed with 9 µL of milli-Q water. In a 96-well plate BSA and protein samples were loaded in duplicate. 200 µL/well of the BCA Reagent was added and the plate was incubated at 37ºC for 30 minutes. Absorbance was measured at 562 nm using the PowerWave XS Microplate Spectrophotometer (BioTek). The same protein concentration was achieved in all samples adding milli-Q water and Laemmli Loading buffer 5x.

Protein lysates with Laemmli buffer 1x were boiled at 96ºC for 5 minutes for protein denaturation. The boiled samples were subjected to SDS-PAGE. The proteins were resolved either in homemade acrylamide gels or in Criterion™ XT Precast gels (4-12% acrylamide, 12+2 well comb). Homemade gels (stacking 5% and resolving 10% acrylamide) were prepared as described in Table 2.

Table 2. Recipes used for preparing homemade acrylamide gels.

	Running gel (10%)	Stacking gel (5%)
30% Acrylamide	10 %	5 %
Tris (1.5 M, pH=8.8)	25 %	25 %
10% SDS	1 %	1 %
10% APS	1 %	1 %
TEMED	0.04 %	0.04 %
Milli-Q water	Up to final volume	Up to final volume

In the case of homemade gels, the proteins were stacked at 90V for 15 minutes and resolved at 150V for 1 hour and 15 minutes in Tris/Glycine buffer. In the case of precast gels, proteins were resolved at 180V for 1 hour and 30 minutes in MOPS buffer. Pink pre-stained protein marker (Nippon MWP02, DDBiolab) was used as a protein weight marker. Then, proteins were transferred to nitrocellulose membranes at 100V during 1 hour (for homemade gels) or 80V during 1 hour and 30 minutes (precast gels) in transfer buffer. Membranes were blocked with 5% non-fat milk prepared in Tris-buffered saline solution containing 0.01% Tween-20 (TBST) for 1 hour.

Primary antibodies were prepared in TBST with 0.002% sodium azide and incubated with the membranes overnight at 4ºC. All antibodies were used at a 1:1000 dilution, except β-Actin (1:2000). Membranes were then washed 3 times (10 minutes each) with TBST and were incubated with the secondary antibody diluted 1:4000 in 5% non-fat milk for 1 hour at room temperature. After that, membranes were washed again 3 times with TBST and developed with Clarity™ Western ECL Substrate (Bio-Rad). Proteins were visualized using the Chemidoc Imaging system. The antibodies used are presented in Supplementary Table 3.

3.4. Statistical analysis:

GraphPad Prism 8 software was used for statistical analysis. In all experiments the confidence level used was 95% (α =0.05). *n* values represent the number of independent experiments performed. One sample *t* test was applied for one-component comparisons with control (hypothetical value=1). In co-culture experiments, for the comparison expected and measured values multiple *t* tests were applied. One-tail statistical analysis was applied for validation of predicted results (hypothesis-driven experiments) and two-tailed statistical analysis was applied for experiment design without predicted result. In the figures presented mean ± standard error of the mean (SEM) is presented.

4. Results

4.1. Characterization of the interferon response on PCa cell line:

The RNA-Seq analysis previously carried out in our laboratory showed an upregulation of the interferon (IFN) signaling transcriptional program in response PGC1α re-expression (Fig. 1A). In order to validate these results, the expression of some IFN-response genes was analyzed 6 days after PGC1α induction (Fig. 1B). For the benefit of having a comprehensive view, the data previously obtained in the lab were also included in the figure. Our results confirm the upregulation of the IFN signaling previously observed, reassuring that PGC1α is capable of driving an interferon transcriptional response.

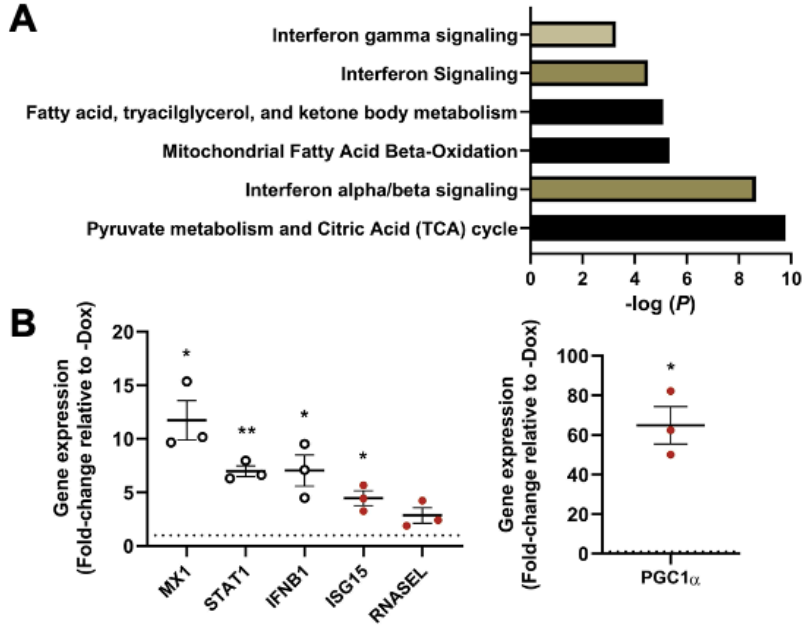

Figure 1. PGC1α upregulates the IFN signaling transcriptional program *in vitro* in PC3 cells. **(A)** RNA-Seq enrichment analysis of the transcriptional program upregulated by PGC1α. **(B)** qRT-PCR gene expression analysis of IFN-response genes and PGC1α after a 6 day Dox treatment (n=3). Data are represented as fold-change relative to -Dox cells, depicted as a dotted line. The data represented in white dots were obtained previously in the lab. *: p-$value < 0.05$; **: p-$value < 0.01$.

Next, we wondered if this IFN signaling was mediating the anti-proliferative effect of PGC1α. But first, we aimed to proof the biological effect of IFN treatment on PC3 cells. In order to do so, PC3 cells were treated with three different concentrations of human recombinant IFN-β (25, 125 and 250 pM). The growth of IFN-β treated PC3 cells was measured at days 3 and 6. Our results show that IFN-β has a significant anti-proliferative effect in a doses-dependent manner (Fig. 2A). Furthermore, the morphology of the cells was also evaluated in response to the drug treatment. Membrane prolongations appeared and stress granules became more apparent after 3 days of treatment (Fig. 2B). With these results we confirm the anti-proliferative effect of IFN-β on PC3 cells and further supports our hypothesis that this could be one of the pathways through which PGC1α modulates cell proliferation.

Once characterized the anti-proliferative effect, we asked if in addition to proliferation, IFN-β treatment could phenocopy PGC1α-induced transcriptional program. For gene expression analysis we used the intermediate concentration of IFN-β, 125 pM. We evaluated the gene expression changes induced by IFN-β at 8, 24 and 72h of treatment in PC3 cells (Fig. 2C). IFN-β treatment upregulated the expression of IFN-response genes at early time-points (8 and 24h) and these transcriptional changes were not maintained over time (72h) (Fig. S1). The genes upregulated in the RNA-Seq analysis were also upregulated in treated cells, showing that IFN-β activates the same transcriptional program induced by PGC1α. Out of all the IFN-response genes analyzed, some of them were not upregulated, suggesting that the doses used were not enough for their overexpression or they are not responsive to IFN-β, but to other IFN type I cytokines. However, some genes such as *MX1*, *ISG15* or *OAS1* showed an early (8h) and significant upregulation in response to IFN-β, pointing out that these genes could be the earliest reporters of an IFN signaling activation in PC3 cells out of all of the IFN-response genes analyzed.

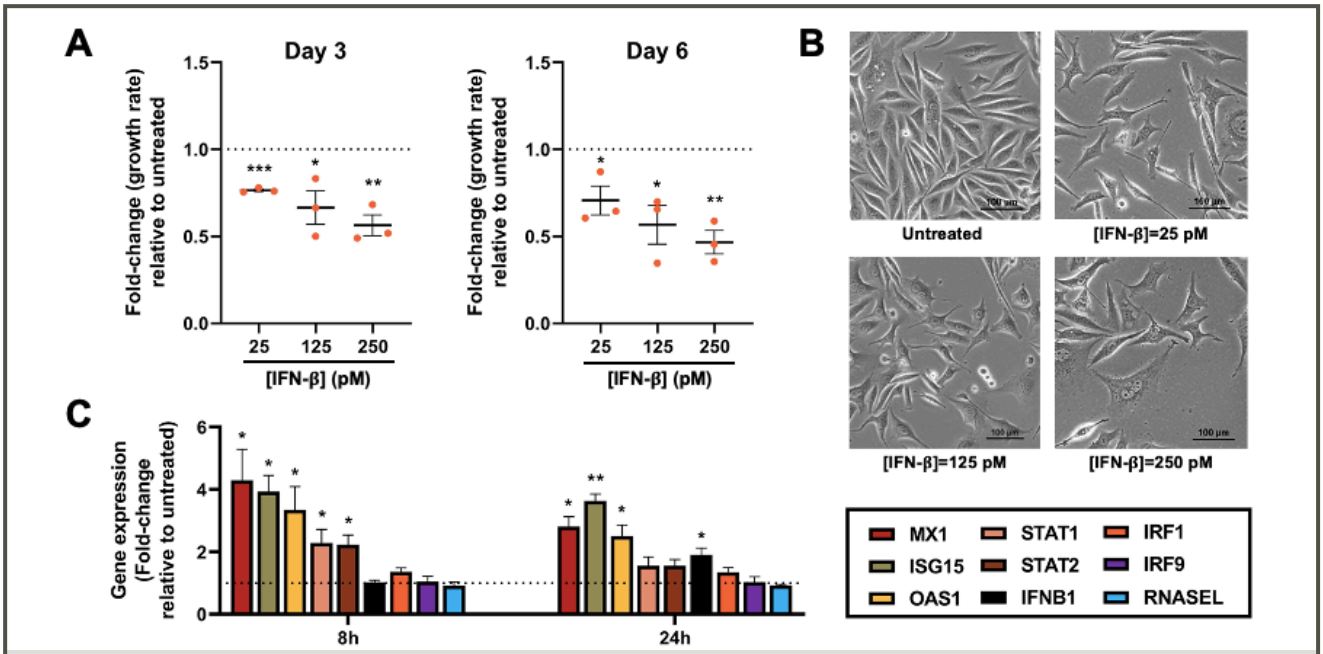

Figure 2. IFN-β modulates cell proliferation and activates IFN signaling transcriptional program in PC3 cells *in vitro*. **(A)** Effect of IFN-β (25, 125 and 250 pM) on the growth rate of PC3 cells at 3 and 6 days post-treatment relative to untreated cells (*n*=3). **(B)** Optical microscopy photographs representative of the changes in cell morphology 3 days after treatment. **Bar scale:** 100 µm. **(C)** qRT-PCR gene expression analysis of IFN-response genes at 8 and 24h after an IFN-β treatment (125 pM) (*n*=3). Data are represented as fold-change relative to untreated cells, depicted as a dotted line. *: *p-value* < 0.05; **: *p-value* < 0.01; ***: *p-value* < 0.001.

4.2. Tracking the PGC1α-driven molecular events over time:

The phosphorylation and further dimerization of STAT1 and STAT2 leads to the formation of the ISGF3 complex (together with IRF9), which migrates to the nucleus and activates the IFN response transcriptional program[13]. Therefore, we sought to interrogate whether the expression of PGC1α could trigger the phosphorylation of STAT1, and the subsequent activation of the IFN signaling program. In order to do so, phospho-STAT1 (P-STAT1) was analyzed 6 days after Dox treatment on PC3 PGC1α cells (Fig. 3A). Our results show a significative increase in P-STAT1 protein level, suggesting that PGC1α promotes the phosphorylation of STAT1. Aiming to track the different molecular events over time, a Dox treatment time-course (16, 24 and 48h) was performed (Fig. 3B, C).

Our results confirm the decrease in c-MYC protein level previously characterized[10] and show an increase in P-STAT1 protein level at 16h after PGC1α overexpression, that is maintained at 24h and 48h. Although these results indicate that the phosphorylation of STAT1 occurs early in time, it is preceded by the downregulation of c-MYC, which occurs at a transcriptional level only 2h after PGC1α expression. In order to study if this early activation of IFN pathway was accompanied by an activation of a transcriptional response, four IFN-response genes were selected: *STAT1*, *IRF1*, *MX1* and *ISG15*; these last two being considered early target genes as our previous results suggested. Although at 16 and 24h there was an uncertain *MX1* upregulation, at 48h this overexpression became significant. These data, together with the upregulation observed at 6 days after the expression of PGC1α, suggest that PGC1α is capable of driving an IFN response signaling mediated by the phosphorylation of STAT1, starting to activate this transcriptional program 48h after its re-expression.

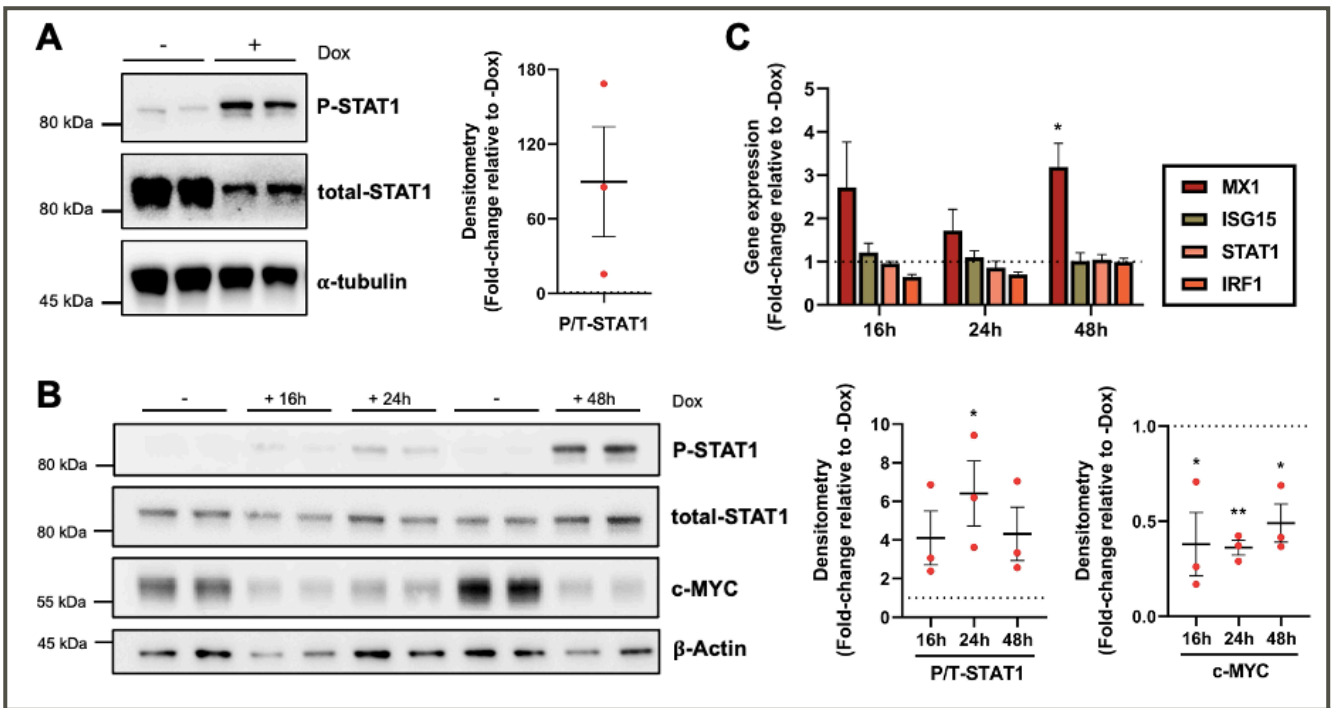

Figure 3. PGC1α activates IFN signaling response 48h after its re-expression in PC3 cells. **(A)** Representative Western blot analysis and quantification of the effect of PGC1α on STAT1 phosphorylation 6 days after its re-expression (*n*=3). **(B)** Representative Western blot analysis and quantification of the effect of PGC1α on STAT1 phosphorylation and c-MYC 16, 24 and 48h after its re-expression (*n*=3). **(C)** qRT-PCR gene expression analysis of IFN-response genes *IRF1*, *STAT1*, *MX1* and *ISG15* 16, 24 and 48h after PGC1α induction (*n*=3). Data are represented as fold-change relative to -Dox, depicted as a dotted line. *: *p-value* < 0.05, **: *p-value* < 0.01.

4.3. Studying the connection between c-MYC and IFN pathway driven by PGC1α:

The decrease in c-MYC driven by PGC1α has previously been demonstrated to have tumor suppressive activity and the silencing of this transcription factor partly phenocopies the effect of PGC1α[10]. Once we demonstrated an upregulation of the IFN pathway driven by PGC1α, we wondered if the decrease in c-MYC (see Fig. 3B) could be mediating these transcriptional changes. In order to explore this possible connection, we studied the expression of three IFN-response genes in PC3 shMYC cells (Fig. 4). Our results showed an increase in the expression of these genes in response to the downregulation of *MYC*, although not statistically significant. These changes in the gene expression support the hypothesis that a PGC1α-driven downregulation of c-MYC positively modulates the IFN transcriptional program, as a part of its tumor suppressive activity. However, the data obtained are not enough to demonstrate a solid connection.

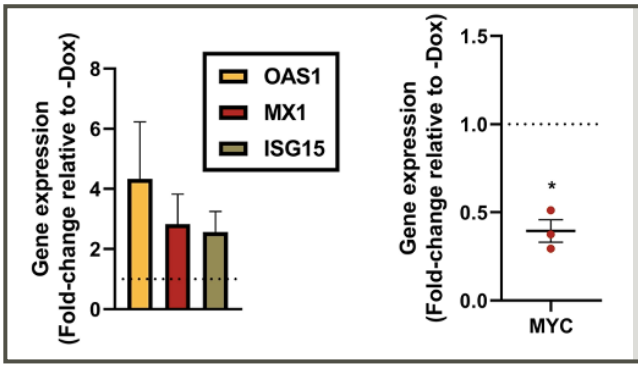

Figure 4. Silencing the transcription factor c-MYC upregulates an IFN signaling response 6 days after its downregulation in PC3 cells. qRT-PCR gene expression analysis of three IFN-response genes: *MX1*, *ISG15* and *OAS1* (*n*=3). Data are represented as fold-change relative to -Dox, depicted as a dotted line. *: *p-value* < 0.05.

4.4. Exploring the extrinsic biological effects of PGC1α:

Previous studies of our laboratory showed an anti-proliferative activity associated with the secretome produced by PGC1α expressing PC3 cells. Additional studies also demonstrated an increase of IFN-β in this secretome. In these experimental settings, secretome producer cells and recipient cells were never in contact. This idea led us to ask if this growth inhibitory response could be transmitted in a paracrine manner in a context closer to the physiological one. In order to further decipher the communication between aggressive (PGC1α-) and non-aggressive (PGC1α+) PCa cells, co-culture experiments were designed. PC3 mCherry was chosen as the aggressive cell line and PC3 PGC1α was chosen as the non-aggressive cell line. PC3 TRIPZ cells were used as a control, with the aim of ensuring that the outcome of the experiments could not be attributed to doxycycline treatment and/or the fact of mixing and culturing two different cell lines.

Three different percentages of co-culture conditions (**PC3 mCherry**:PC3 PGC1α cells or PC3 TRIPZ cells) were studied (**80**:20, **50**:50 and **20**:80). Growth rates at days 3 and 6 were calculated as relative to day 0 for each condition (Fig. 5). In this first assay the overall growth of each co-culture condition was measured. The growth rate of each cell line was also determined in monocultures. Taking into account the growth rate of each cell line (monocultures) and the composition of each co-culture condition, expected growth rates were calculated for days 3 and 6. These expected growth rates represent the overall proliferation of each co-culture condition if cells grew independently, without any communication that could alter their proliferation. As anticipated, the overall growth rate decreases as the proportion of PC3 PGC1α cells increases, due to the slower growth rate of PC3 PGC1α cells (~3.5 times lower than PC3 mCherry cells at Day 6; not shown). In the case of PC3 TRIPZ co-cultures, the growth rate seems to be identical (n.s.) independent of the condition of study. The measured (real) growth rates were compared to the expected (calculated) ones. Results show no difference between the expected proliferation and the one measured in any of the different conditions. Therefore, these data suggest that the cell growth measured and the one expected if PC3 PGC1α (PGC1α+) and PC3 mCherry (PGC1α-) cells grew independently is the same.

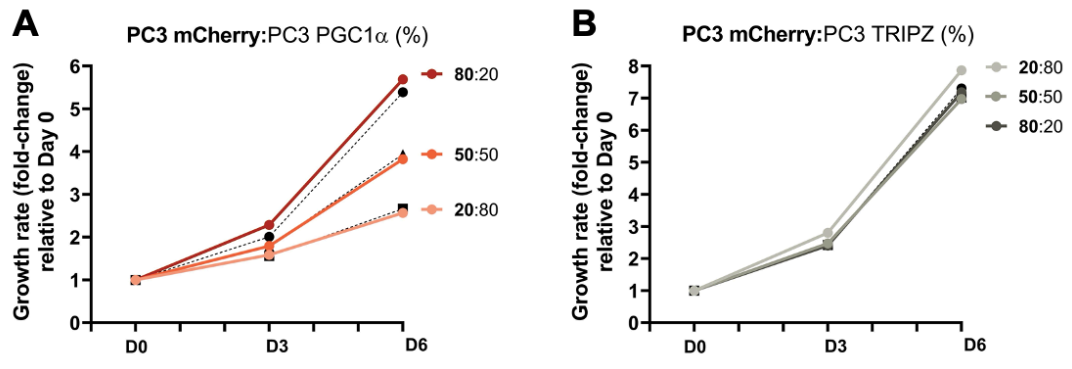

Figure 5. Growth rate (fold-change) relative to Day 0 in different co-culture conditions. Growth evolution is shown for **(A)** the different co-cultures of PC3 mCherry and PC3 PGC1α cells and **(B)** the different co-cultures of PC3 mCherry and PC3 TRIPZ cells (*n*=4). Black dotted lines represent the expected growth rate for each co-culture condition, calculated from the growth rate of each cell line in monocultures. **D0**: Day 0; **D3**: Day 3; **D6**: Day 6.

Once studied the overall proliferation of the co-cultures, we were interested in following the percentage (%) of each cell population (PC3 mCherry and PC3 PGC1α) at the same time points previously studied (days 3 and 6) and at day 9 as an exploratory approach (n=1). As did before, taking into account the growth rate of each cell line (monocultures) and the composition of each condition, the expected % of each population was calculated for days 3 and 6. These expected data were compared with the data obtained in the flow cytometry assays, representing the time evolution of the % PC3 mCherry cells in the time course of 9 days (Fig. 6A).

The evolution of the % of PC3 mCherry cells in co-cultures reflects the growing tendency of this cell population. The growing behavior of these aggressive cells (and consequently of the non-aggressive ones) was different from the one expected. We distinguished two clear growing tendencies when compared the measured % PC3 mCherry and expected % PC3 mCherry cells (Fig. 6B). From D0 to D3, the percentage increase per day was significantly higher than expected; showing that during these first three days, the aggressive PCa cells proliferated more than expected if they grew in monoculture conditions. On the other hand, from D3 to D6, the percentage increase was significantly lower than the expected one; showing that during the following three days, the aggressive cells were proliferating slower than they would if they were in monoculture conditions.

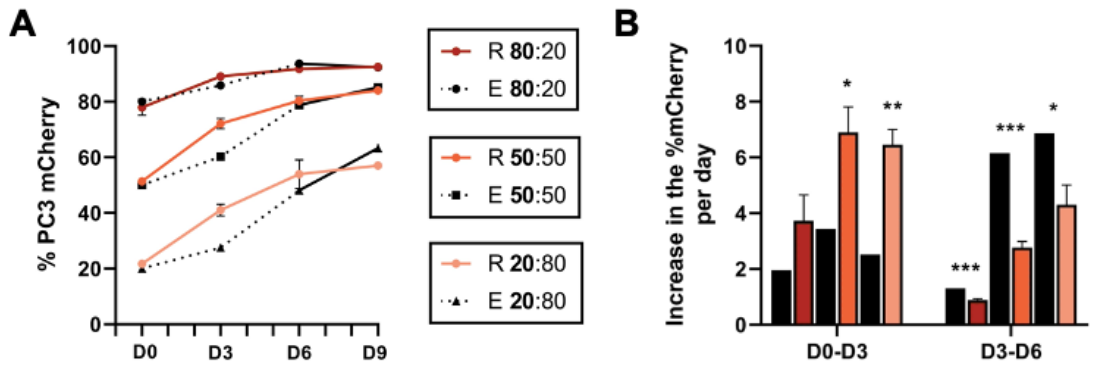

Figure 6. (A) Measured time evolution of the % PC3 mCherry cells through the course of 9 days. The measured % PC3 mCherry cells is shown in solid color lines for the three different co-culture conditions, while the expected % is shown in black dotted lines (n=3). The evolution of each condition from D6-D9 was studied without changing the medium (color lines) or discarding the medium and adding fresh one on days 3 and 6 (black solid lines); exploratory (n=1). **(B)** Increase in the % PC3 mCherry cells per day. The increase measured is shown in color bars and the expected one in black bars, for the two different time zones: D0–D3 and D3–D6. *: *p-value* < 0.05; **: *p-value* < 0.01; ***: *p-value* < 0.001. **D0**: Day 0; **D3**: Day 3; **D6**: Day 6.

5. Discussion

Interferons, which are cytokines not only produced by tumor cells but also by the microenvironment, have shown to be capable of exerting a direct tumor-suppressive effect on tumor cells by modulating proliferation, differentiation, migration and antigen presentation[13,14]. In PCa the role of these cytokines has not been completely studied. A previous study on 118 PCa patients has reported that low-score values for IFN-β in prostate tumors were significantly associated with biochemical recurrence and worse prognosis[14]. Furthermore, a study of Shou and colleagues demonstrated that IFN pathway is indeed suppressed when benign PCa cells become tumorigenic[15]. Altogether these studies highlight the relevance of unravelling the role of these

cytokines and their associated signaling pathway in prostate cancer, driven by the necessity of biomarkers and gene signatures capable of stratifying patients.

In order to verify that IFN pathway activated by PGC1α drives its anti-proliferative effect, we first needed to assess the anti-proliferative effect of the cytokine itself in our cell system. When studied the IFN transcriptional program activated in response to IFN-β treatment, the upregulation was not the same for all the IFN-response genes analyzed. Three out of the nine canonical IFN type I genes studied were not upregulated (*IRF1*, *IRF9* and *RNASEL*). These data could be explained either because the concentration used was not enough for their overexpression or because they might not be responsive to IFN-β but to other IFN type I cytokines. Nevertheless, we consider the data obtained a good validation, demonstrating the link between IFN pathway and its growth inhibitory effect on PCa PC3 cells. Moreover, our results are in line with another study that has previously supported the tumor suppressive activity of IFN-β in PC3 cells at the same IFN-β doses tested[16].

Once studied the biological effect of IFN signaling and characterized the upregulation of IFN-response genes, both in treated cells and PGC1α-expressing cells, we aimed to track over time the molecular events triggered by the re-expression of PGC1α. The significant increase in P-STAT1 protein level 6 days after PGC1α induction was in line with our previous IFN-response genes expression data, which led us to propose that the IFN transcriptional program was driven by PGC1α possibly through the phosphorylation of STAT1, a novel molecular mechanism yet unknown. Nonetheless, in the results presented in Fig. 3A there is a decrease in total-STAT1 in response to PGC1α expression. This result is inconsistent with the previously characterized upregulation of *STAT1* at mRNA level. In previous Western blots carried out in our laboratory this result was not replicated. Therefore, we propose that this incoherence can be explained by a failed Western blot analysis.

Although our results demonstrate a PGC1α-driven phosphorylation of STAT1 as early as at 16h, there was some uncertainty in the time-point at which an increase in P-STAT1 protein level occurs. Complementary to the time-course experiments presented, we performed a short time-course analyzing both gene and protein expression at 2, 4, 6 and 8h after PGC1α induction. The results were not conclusive, showing an increase in the phosphorylation of STAT1 at 8h in only two of the three experiments carried out. Together with the upregulation of *MX1* at 48h after PGC1α re-expression, we propose this time-point as the beginning of the IFN transcriptional program observed at 6 days after PGC1α induction.

Our data suggest that the PGC1α-driven STAT1 phosphorylation could trigger molecular events that induce the IFN transcriptional program and the subsequent growth inhibitory response observed. This molecular mechanism has not been previously reported in the literature, demonstrating the molecular complexity of the pathways modulated by the tumor-suppressor PGC1α in PCa. A previous study has uncovered a defective IFN-JAK-STAT1 signaling pathway in PCa cells that was inactivated in a MYC-dependent manner[20]. Together, our preliminary data suggest that the tumor suppressive response of PGC1α is associated with the downregulation of c-MYC and the subsequent upregulation of the IFN pathway in PCa cells. A possible molecular mechanism for the activation of the IFN transcriptional program is a MYC-dependent activation of JAK or TYK kinases, mediating the phosphorylation of STAT1.

Through the co-culture experiments we aimed to study the biological effect of cell communication between PGC1α expressing and non-expressing PCa cells. The change in the growing tendency of PCa aggressive cells reflects an anti-proliferative response three days after seeding. According to previous studies of the lab and our last data, we hypothesize that during these first three days there is an upregulation of the characterized PGC1α-driven IFN pathway and a change in the secretome composition produced by PGC1α expressing cells. The accumulation of these secretome components in the culture medium during the first three days could be driving the growth inhibitory effect observed in aggressive cells in the following days. Moreover, striving to eliminate the secretome component, two different conditions were seeded and harvested on day 9. In the first one, the culture medium was replaced with fresh one every three days; while in the other one the medium was not changed. In the co-culture conditions where the medium was changed, a remarkable increase in the % of aggressive PCa cells was observed. Although additional experiments are required in order to provide consistent results, these preliminary results support our hypothesis, remarking the importance of the extrinsic effects of the re-expression of PGC1α. The pro-proliferative effect of PCa aggressive cells during the first three days was a novel and previously unexplored response. Additional controls using co-cultures of aggressive cells should be carried out. The pro-proliferative behavior of PCa aggressive cells in the first three days balances the anti-proliferative behavior of the next three days (see Fig. 6A at D6), explaining how there were no differences in the overall growth rate of the co-culture.

Numerous studies have shown the ability of IFNs to modulate tumorigenesis in an paracrine manner exerting a tumor suppressive response and stimulating immune cytotoxic cells[13,14]. The extrinsic mechanisms of PGC1α contribute to its tumor suppressive activity and we hypothesize that IFN pathway can ultimately be transmitted in a paracrine manner, modulating the tumor microenvironment and opposing the progression of the disease.

6. Future directions and Conclusions

The molecular mechanism through which PGC1α promotes the phosphorylation of STAT1 and the activation of IFN transcriptional program is yet unknown. In order to explore this mechanism, it would be interesting to chemically inhibit the receptor associated kinases (JAK1 or TYK2) that drive the phosphorylation of STAT1 or genetically silence *IRF9*, necessary for the formation of the ISGF3 complex. These experimental settings would allow us to better describe the role of PGC1α in the activation of this signaling pathway. In addition, we consider necessary to measure P-STAT2 protein level in response to PGC1α induction. Owing to the fact that some of the upregulated genes are exclusively modulated by IFN type I cytokines through the formation of the ISGF3 complex, we expect an increase in the phosphorylation of STAT2 driven by PGC1α. Studying the upregulated IFN type II (IFN-γ)-response genes would also be interesting, due to the plausible synergistic effects of IFN type I and II response genes involved in the tumor suppressive effect of PGC1α.

The link between PGC1α-driven IFN pathway and the downregulation of c-MYC is an interesting novel mechanism that needs to be further studied. In order to statistically confirm the upregulation of IFN-response genes in response to *MYC* downregulation, a higher number of experiments is required. Although this approach is a good start, our hypothesis needs to be further supported by a downregulation of the IFN pathway in response to the rescue of *MYC* expression in PGC1α expressing PCa cells.

Related to the extrinsic mechanisms of PGC1α there are many aspects to shed light on. Although in this work we only characterized the biological effect of a paracrine communication between PGC1α expressing and non-expressing PCa cells, we consider necessary to study the underlying molecular mechanisms. In order to do so, a Fluorescence-Activated Cell Sorting (FACS) experiment can be designed, in which aggressive (mCherry+) and non-aggressive cells could be separated. After doing so, we could study the IFN pathway with or without changing the culture medium in aggressive PCa cells at the different time-points analyzed.

On the grounds of all these data, IFN-β and its associated signaling pathway are potent candidates for the development of antitumor drugs; however, recombinant IFN-β is too unstable to be used in therapy *in vivo*[14]. Moreover, clinical trials of immunotherapy for advanced PCa using IFN type I cytokines (IFN-α or IFN-β) have been shown not to be effective and in some cases, capable of inducing severe toxicity[21]. Therefore, new strategies need to be taken into account in order to present prognostic or clinical value. We consider the present work a first approach to studying the link between IFN pathway and the tumor-suppressive properties of PGC1α in PCa, offering potential for new therapeutic targets and strategies.

7. References:

1. Bray F, et al. Global Cancer Observatory: Cancer Today. Lyon, France: International Agency for Research on Cancer. 2020. Accessed June 4, 2021. https://gco.iarc.fr/today

2. Lilja H, Ulmert D, Vickers AJ. Prostate-specific antigen and prostate cancer: Prediction, detection and monitoring. *Nat Rev Cancer*. 2008;8(4):268-278. doi:10.1038/nrc2351

3. Wang G, Zhao D, Spring DJ, DePinho RA. Genetics and biology of prostate cancer. *Genes Dev*. 2018;32(17-18):1105-1140. doi:10.1101/gad.315739.118

4. Weinberg RA, et al. Hallmarks of cancer: The next generation. *Cell*. 2011;144(5):646-674. doi:10.1016/j.cell.2011.02.013

5. Torrano V, Valcarcel-Jimenez L, Cortazar AR, et al. The metabolic co-regulator PGC1α suppresses prostate cancer metastasis. *Nat Cell Biol*. 2016;18(6):645-656. doi:10.1038/ncb3357

6. Bost F, Kaminski L. The metabolic modulator PGC-1α in cancer. *Am J Cancer Res*. 2019;9(2):198-211.

7. Finck BN, Kelly DP. PGC-1 coactivators: Inducible regulators of energy metabolism in health and disease. *J Clin Invest*. 2006;116(3):615-622. doi:10.1172/JCI27794

8. LeBleu VS, O'Connell JT, Gonzalez Herrera KN, et al. PGC-1α mediates mitochondrial biogenesis and oxidative phosphorylation in cancer cells to promote metastasis. *Nat Cell Biol*. 2014;16(10):992-1003. doi:10.1038/ncb3039

9. Andrzejewski S, Klimcakova E, Johnson RM, et al. PGC-1α Promotes Breast Cancer Metastasis and Confers Bioenergetic Flexibility against Metabolic Drugs. *Cell Metab*. 2017;26(5):778-787. doi:10.1016/j.cmet.2017.09.006

10. Valcarcel-Jimenez L, Macchia A, Crosas-Molist E, et al. PGC1a suppresses prostate cancer cell invasion through ERRA transcriptional control. *Cancer Res*. 2019;79(24):6153-6165. doi:10.1158/0008-5472.CAN-19-1231

11. Dejure FR, Eilers M. MYC and tumor metabolism: chicken and egg. *EMBO J*. 2017;36(23):3409-3420. doi:10.15252/embj.201796438

12. Wongvipat J, et al. Myc-driven murine prostate cancer shares molecular features with human prostate tumors. *Cancer Cell*. 2005;8(6):485. doi:10.1016/j.ccr.2005.11.010

13. Parker BS, Rautela J, Hertzog PJ. Antitumour actions of interferons: Implications for cancer therapy. *Nat Rev Cancer*. 2016;16(3):131-144. doi:10.1038/nrc.2016.14

14. Fernandez-Garcia B, et al. Analysis of the expression of interleukins, interferon β, and nuclear factor-κ B in prostate cancer and their relationship with biochemical recurrence. *J Immunother*. 2014;37(7):366-373. doi:10.1097/CJI.0000000000000045

15. Gao WQ, et al. Expression profiling of a human cell line model of prostatic cancer reveals a direct involvement of interferon signaling in prostate tumor progression. *Proc Natl Acad Sci U S A*. 2002;99(5):2830-2835. doi:10.1073/pnas.052705299

16. Angelucci C, et al. Recombinant human IFN-β affects androgen receptor level, neuroendocrine differentiation, cell adhesion, and motility in prostate cancer cells. *J Interf Cytokine Res*. 2007;27(8):643-652. doi:10.1089/jir.2006.0120

17. Pettaway C, et al. Suppression of angiogenesis, tumorigenicity, and metastasis by human prostate cancer cells engineered to produce interferon-β. *Cancer Res*. 1999;59(4):872-879.

18. Arreal L, et al. Targeting PML in triple negative breast cancer elicits growth suppression and senescence. *Cell Death Differ*. 2020;27(4):1186-1199. doi:10.1038/s41418-019-0407-5

19. Solera J, et al. Real-time PCR detection chemistry. *Clin Chim Acta*. 2015;439:231-250. doi:10.1016/j.cca.2014.10.017

20. Yu Q, et al. EZH2-mediated inactivation of IFN-γ-JAK-STAT1 signaling is an effective therapeutic target in MYC-driven prostate cancer. *Cell Rep*. 2014;8(1):204-216. doi:10.1016/j.celrep.2014.05.045

21. Haas GP, et al. Clinical trials of immunotherapy for advanced prostate cancer. *Urol Oncol*. 2000;5(6):265-273. doi:10.1016/S1078-1439(00)00086-7

Supplementary Data:

Supplementary T1. Composition of the buffers used.

Buffer	Composition
RIPA buffer	50 mM TrisHCl pH 7.5, 150 mM NaCl, 1 mM EDTA, 0.1% SDS, 1% Nonidet P40, 1% sodium deoxycholate, 1 mM sodium fluoride, 1 mM sodium orthovanadate, 1 mM betaglycerophosphate and protease inhibitor cocktail (Roche)
Laemmli Loading buffer	10% SDS, 50 mM Tris pH 6.8, 10% H_2O, 50% glycerol, 1% β-mercaptoethanol, 10 mM DTT and 0.2 mg/mL of bromophenol blue
Transfer buffer	200 mM glycine, 25 mM Tris, 20% ethanol and milli-Q water up to volume

Supplementary T2. Information about the primer sequences.

Gene	Species	Left primer sequence	Right primer sequence
Pgc1a	Mouse	GAAAGGGCCAAACAGAGAGA	GTAAATCACACGGCGCTCTT
GADPH	Human	ACATCGCTCAGACACCATG	TGTAGTTGAGGTCAATGAAGGG
MX1	Human	GAAAGAGGCGAAGCGAGAG	CCGTGACACTGGGATTCCT
ISG15	Human	CGAACTCATCTTTGCCAGTACA	GCCTTCAGCTCTGACACC
OAS1	Human	GTGAGCTCCTGGATTCTGCT	AGGGTACTCATGTGTTCCAATGT
STAT1	Human	GAGCTTCACTCCCTTAGTTTTGA	CACAACGGGCAGAGAGGT
STAT2	Human	TGCAGTTCCTCTGTCACACC	GGTTTGATTTGGGACTTTGGT
IFNB1	Human	CTTTGCTATTTTCAGACAAGATTCA	GCCAGGAGGTTCTCAACAAT
IRF1	Human	GGCACATCCCAGTGGAAG	CCCTTCCTCATCCTCATCTGT
IRF9	Human	AGCCTGGACAGCAACTCAG	GAAACTGCCCACTCTCCACT
RNASEL	Human	AGCAGTCTTCCAGGCTTTG	CAACAGAGCAGCAGTATGAAGA
MYC	Human	TCCTCGGATTCTCTGCTCTC	TCTTCCTCATCTTCTTGTTCCTC

Supplementary T3. Information about the antibodies used.

Protein	Source	Isotype	Reference	UniProt ID	Molecular weight (kDa)
STAT1	Cell Signaling Technology	Rabbit IgG	D1K9Y	P42224	84-91
P-STAT1 (Tyr701)	Cell Signaling Technology	Rabbit IgG	58D6		
c-MYC	Cell Signaling Technology	Rabbit IgG	D3N8F	P01106	57-65
β-Actin	Cell Signaling Technology	Mouse IgG	8H10D10	P60709	45
α-Tubulin	Sigma-Aldrich	Mouse IgG	DM1A	P68366	50

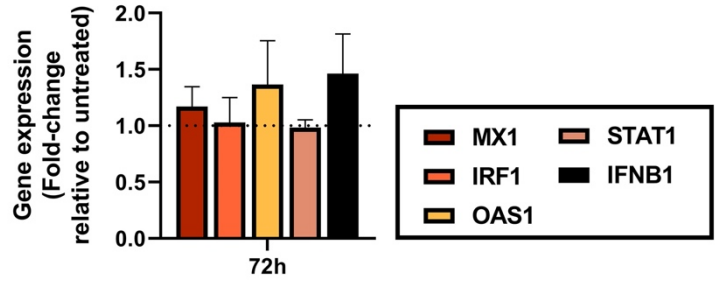

Figure S1. qRT-PCR gene expression analysis of IFN-response genes at 72h after an IFN-β treatment 125 pM (*n*=3; independent experiments). Data are represented as fold-change relative to untreated cells, depicted as a dotted line.